Int. J. Heat Mass Transfer. Vol. 21, pp. 1333–1340

0017-9310/78/1001-1333 $02.00/0

EXPERIMENTAL FREQUENCY DOMAIN DYNAMICS OF HEAT PIPES

A. RAJAKUMAR* and P. R. KRISHNASWAMY
Department of Chemical Engineering, Indian Institute of Technology, Madras—600036, India

(*Received* 11 *October* 1977 *and in revised form* 2 *March* 1978)

Abstract—Detailed frequency response data were obtained experimentally using a number of water heat pipes with compressed bronze screen as the wicking material. The experimentation involved subjecting the heat pipes to step change in heat input and converting the time response data to frequency response via Fourier transformation. Variations in such parameters as operating temperature, condenser area, evaporator area, and wick thickness were achieved in order to study their effects on the system dynamics. The results obtained were compared with a proposed theory to validate the latter. Apart from providing quantitative information on the hitherto unavailable frequency domain dynamics, the results also elucidate the influence of experimental variables on the dynamics.

NOMENCLATURE

A, input step magnitude;
C, heat capacity;
d_0, outside diameter of heat pipe;
d_v, vapor core diameter;
D, $(\alpha_w/\alpha_m)^{1/2}$;
F, forcing function;
$G(s)$, $G(j\omega)$, system transfer function;
h, heat-transfer coefficient;
H, specific enthalpy;
Im, imaginary part of the system transfer function;
j, $(-1)^{1/2}$;
K, thermal conductivity;
L, length;
M_v, mass of vapor occupying the vapor space;
N_{Bi}, Biot number, $h_i y_t/K_m$;
$Q(t)$, rate of heat transfer to the sink;
R, K_m/K_w;
Re, real part of the system transfer function;
s, Laplace parameter;
t, time;
t_y, time at which the response reaches the steady state;
T, temperature;
x, axial coordinate;
$x(s)$, Laplace transform of the system input;
$x(t)$, system input;
X, dimensionless length, x/L_t;
y, transverse coordinate;
$y(s)$, Laplace transform of the system output;
$y(t)$, system output;
y_m, metal wall thickness;
y_t, combined thickness of the wall and the wick;
y_w, wick thickness.

Greek symbols

α, thermal diffusivity;
γ, defined by equation (4a);
ε, wick porosity;
η, dimensionless transverse coordinate, y/y_t;
η_m, dimensionless wall thickness, y_m/y_t;
σ, dimensionless heat flow, $Q(t)/Q_s$;
ϕ, dimensionless temperature, $\pi d_0 L_t K_m T(y,t)/Q_s y_t$;
ω, angular frequency.

Subscripts

c, condenser;
e, evaporator;
i, input;
l, liquid;
m, metal wall;
o, output;
s, steady state;
S, screen;
t, total;
v, vapor;
w, wick.

INTRODUCTION

THE IMPORTANCE of frequency response data in model checking, parameter evaluation, rational system design and optimization of feedback control need hardly be emphasised. Such applications of frequency response, for example, have been extensively illustrated by Hougen [1]. Nonetheless, very little information is available in the literature on frequency domain dynamics of heat pipes. The only published data to date

*Present address: Reactor Research Centre, Kalpakkam 603102, India.

in this area seem to be the ones reported by Gröll and Zimmermann [2] on measured step and sinewave response characteristics of different heat pipes under normal operating conditions. Their results, however, are too limited to provide a detailed knowledge of the system dynamic behaviour. The other available experimental dynamic data on heat pipes essentially deal with aspects of startup [3,4] and transient response [5,6].

It is thus the objective here to provide extensive experimental frequency response data in order to differentiate the influence of heat pipe parameters (such as wick thickness, condenser area, evaporator area, and operating temperature) on its dynamics. Besides, the results will also be used to test the validity of a model proposed earlier by the authors [7].

It is well-known that direct sinewave testing has several practical disadvantages, viz., prolonged test time, repeated experimentation at several discrete frequencies, need for a sinewave generator, and sustained off specification output (varying sinusoidally in quality). To circumvent these problems pulse testing [8,9] was evolved which essentially involves introduction of a nondescript nonperiodic input into the system and transformation of the resulting response into frequency domain. This method, however, is found to give reliable results only in the relatively low frequency region (i.e. below 30 rad/min). The authors [10] have therefore developed a dynamic testing procedure for converting step response data (which are normally easy to obtain experimentally) to frequency response with greater precision and over a considerably wider spectrum of frequencies. This technique is employed here to procure the required heat pipe frequency response.

THEORY

Derivation of the mathematical model employed in this work is indicated elsewhere [7]. Briefly this involves dividing the heat pipe into two radial components (wall and wick) and three axial components (evaporator, adiabatic, and condenser sections). Application of energy balance over these components results in a set of six partial differential equations which are solved via Laplace transform with the aid of appropriate initial and boundary conditions. This procedure yields the transfer functions relating several input–output pairs of variables of interest. Thus, the transfer functions relating vapor temperature, ϕ_v, and heat transfer to the sink, σ_o, to the evaporator and condenser side forcing functions (F_e and F_c) are found to be [7, 11]

$$G_{ve}(s) = \frac{\phi_v(s)}{F_e(s)} = \frac{(N_4G_3 - N_3r_1G_2)G_1G_2X_c}{G(s)} \tag{1}$$

$$G_{vc}(s) = \frac{\phi_v(s)}{F_c(s)} = \frac{(N_2G_3 - N_1r_1G_2)G_1G_2X_c}{G(s)} \tag{2}$$

$$G_{oe}(s) = \frac{\sigma_o(s)}{F_e(s)} = \frac{N_4r_1G_2X_eX_c}{G(s)} \tag{3}$$

and

$$G_{oc}(s) = \frac{\sigma_o(s)}{F_c(s)} = -\frac{r_1G_2X_c\left[N_2X_e + \dfrac{G_1^2(N_2G_3 - N_1r_1G_2)(\gamma G_4 + r_1G_2)}{RD\gamma}\right]}{G(s)} \tag{4}$$

where:

$$G_1 = \cosh r_1\eta_m \cosh r_2(1-\eta_m);$$
$$G_2 = 1 + RD \tanh r_1\eta_m \tanh r_2(1-\eta_m);$$
$$G_3 = \tanh r_1\eta_m + RD \tanh r_2(1-\eta_m);$$
$$G_4 = \tanh r_2(1-\eta_m) + RD \tanh r_1\eta_m;$$
$$G_5 = N_2(N_4G_3 - N_3r_1G_2)X_e + N_4(N_2G_3 - N_1r_1G_2)X_c;$$
$$G_6 = (N_2G_3 - N_1r_1G_2)(N_4G_3 - N_3r_1G_2);$$
$$G(s) = G_5 + \frac{G_1^2G_6(r_1G_2 + \gamma G_4)}{RD\gamma};$$
$$r_1 = (Ds)^{1/2}; \qquad r_2 = (s/D)^{1/2};$$

and

$$\gamma = \left[\frac{K_w(H_{vs} - C_vT_{vs})\pi d_v}{C_vM_{vs}H_{vs}}\right]\frac{L_tY_t}{(\alpha_m\alpha_w)^{1/2}}. \tag{4a}$$

The dimensionless parameters N_1, N_2, N_3 and N_4 in the above equations and the dimensionless form of the forcing functions, F_e and F_c, would depend on the type of boundary conditions employed at the evaporator–condenser outer surface. In other words, from the general results shown above, transfer functions pertinent to specific boundary conditions may be derived. For example, for the case where heat σ_i is supplied by resistance heating and removed by convection (as in our experimentation), it has been shown that [7]

$$N_1 = -X_e, \quad N_2 = 0, \quad N_3 = 1/N_{Bi} = K_m/h_cy_t, \quad N_4 = 1 \tag{5}$$

with the result equation (1) reduces to

$$G_{ve}(s) = \frac{\phi_v(s)}{\sigma_i(s)} = \frac{G_1(G_3 + r_1G_2/N_{Bi})}{r_1X_c\bar{G}} \tag{6}$$

where

$$\bar{G} = 1 + \frac{G_1^2(G_3 + r_1 G_2/N_{Bi})(\gamma G_4 + r_1 G_2)}{RD\gamma X_c}.$$

Similar transfer function equations relating other input–output variables can also be derived [7] for the same or different boundary conditions.

The final equations, such as equation (6), may be converted to theoretical frequency functions by replacing s by $j\omega$ and reducing the resulting ratio of complex numbers to an equivalent amplitude ratio and phase angle. To avoid algebraic complications, this was achieved by coding the transfer function (equation 6) directly in the complex mode and resolving it into real and imaginary parts using the library functions available in our IBM 370/155 computer. The magnitude and phase data thus computed constitute the theoretical frequency response of heat pipes. A discussion on these theoretical results may be found in [7].

EXPERIMENTAL

Apparatus

Six heat pipes were designed and constructed in order to evaluate their dynamic performance via step testing. The experiments were planned to cover important system and operating parameters. All the pipes were of 2.0 cm O.D. thin-walled copper tubing with a working length of 42.0 cm. Provisions were made to vary the evaporator length from 11 to 32 cm and the condenser length from 10 to 21 cm. Compressed wicks in three different thicknesses (viz. 0.25, 0.70 and 1.20 mm) composed of multilayered phosphor bronze (95% Cu) screens of either 150 or 250 mesh size were employed. Each observed wick thickness resulted from averaging 16 measurements made along the pipe length with a travelling vernier microscope having a sensitivity of ± 0.01 mm and this amounted to less than 8% error in y_w data. Water was chosen as the working fluid in view of its compatibility with copper and availability in pure form.

Extreme care was taken to clean the pipe and wick material thoroughly before assembly. A good thermal contact between the container inner surface and the wick lining was achieved by adopting the following fabrication procedure. The clean wire mesh was first wrapped tightly several times around a carefully machined and highly polished stainless steel rod such that, when inserted, it just fitted into the copper pipe. The entire assembly was then drawn under pressure through a die to compress the wick layer. The stainless steel rod was then removed simply by tapping it with a mallet. The resulting wick structure formed a cold mechanical bonding with the inside surface of the tube and was found to be rigid and uniform throughout. Fitting of two machined end caps with provisions to connect a thermocouple at one end and a vacuum system at the other completed the construction. The heat pipe was then leak-tested and equipped with heating and cooling arrangements.

A schematic of the overall experimental setup is shown in Fig. 1. It essentially consists of the heat pipe, a Laybold vacuum pump, and associated measuring and recording instrumentation for temperature, heat input and vacuum. Heat supply, uniformly distributed over the evaporator zone, was effected by means of a nichrome resistance heater rated at 200 W. Two heaters, one 10 cm long and the other 21 cm, were employed in this study. The energy input was regulated through a variable transformer and measured using a voltmeter and an ammeter. The heating element and

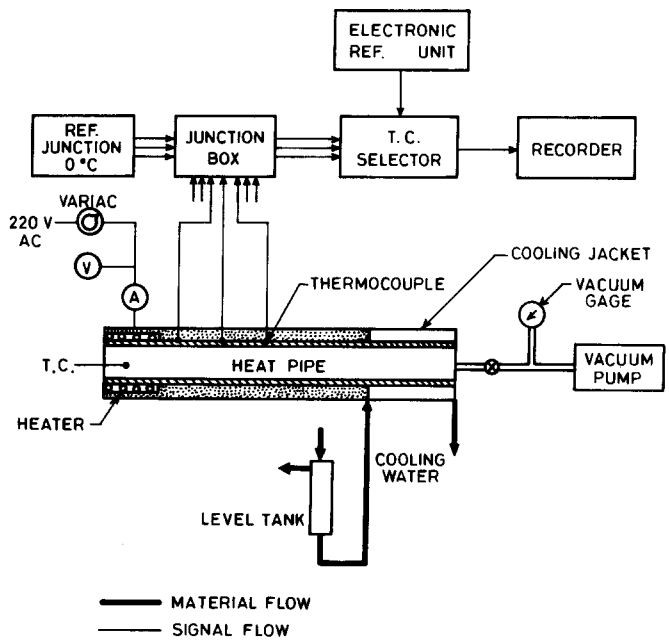

FIG. 1. Schematic of the experimental setup.

the adjoining adiabatic section were thoroughly insulated.

Heat rejection was achieved by natural convection or by a water-cooled jacket. Natural convection was extensively used because it offered a convenient means of studying the effect of condenser length variation. The cooling jacket, separated from the heat pipe by an air gap so as to reduce the temperature gradient across the wick and the wall, was annular in construction.

The heat pipe was instrumented with twelve copper constantan thermocouples. Two thermocouples recorded the temperatures of the inlet and outlet coolant flow, one the ambient temperature and another one measured the vapor temperature at a distance of 5 cm away from the evaporator end. The remaining eight thermocouples were located along the pipe surface at equidistant spacing. Leads from the thermocouples were run to a junction box and through an automatic selector switch to a 12-point multispeed recorder. To make optimum use of the available recorder sensitivity of 2 mV for a full scale deflection of 21 cm (representing an error of 0.7% in temperature data) and to record all levels of temperature measurement in one single range, appropriate biasing potentials were applied to the thermocouple outputs from an electronic reference unit. The time constant of the measuring and recording devices and that of the heater element were found to be negligible (<3.0 s) compared to the system time constant of about 14 min.

Procedure

The heat pipe was loaded with proper amount of distilled water (as so to saturate the wick), evacuated, sealed, and disconnected from the vacuum system. In experiments involving forced cooling, the condenser coolant flow was adjusted to the required level by a valve in the coolent flow line. Power input to the evaporator, as monitored by the ammeter and voltmeter, was maintained at a predetermined value by adjusting the variable transformer. The system was thus allowed to reach the desired steady state. Attainment of uniform evaporator surface temperatures (equalling the saturation temperature) was an indication of proper system operation.

Power variation to the heater, in the form of a step of desired magnitude, was then introduced by suddenly turning the transformer dial to a preselected value. The resulting surface temperature changes along the length and the vapour and coolant temperature variations were recorded. Several laboratory experiments were performed using different heat pipes at different temperature levels of operation. The ranges of experimental variables covered are: operating temperature: 35–100°C; evaporator length: 24–50% of total length; condenser length: 26–76% of total length; wick thickness: 1.23–5.9% of pipe diameter.

For the purpose of comparing experimental data with theoretical predictions, an estimate of wick properties (namely porosity and thermal conductivity) was needed. These properties data were evaluated as follows.

The wick porosity was determined following the procedure given by Cosgrove [12]. This involves determining the volume of water required to completely fill the heat pipe. From a knowledge of the volume of the vapor core, the porosity could then be easily computed.

For estimating the thermal conductivity, K_w, of the liquid-filled wicks, widely varying methods [13–16] were found in the literature. In the absence of reliable conductivity data, lower bound given by the series conduction path is recommended [16]. Accordingly the series conduction path formula

$$K_w = \frac{K_1 K_S}{\varepsilon K_S + (1-\varepsilon) K_1} \tag{7}$$

was employed here for K_w. It may be noted that values thus obtained agreed closely with those predicted by Gorring and Churchill equation [13].

Data reduction

The recorded time response data were converted to frequency response via the procedure developed earlier [10]. This involves defining the system transfer function, relating the observed system input $x(t)$ and the corresponding output $y(t)$, as

$$G(s) = \frac{y(s)}{x(s)} = \frac{sy(s)}{sx(s)} = \frac{\int_0^{t_y} y'(t)\,e^{-st}\,dt}{\int_0^{t_x} x'(t)\,e^{-st}\,dt}. \tag{8}$$

It may be recalled that multiplication of the numerator and the denominator by s in the above equality amounts to differentiation of the time response data as indicated by the prime inside the integrals. For a perfect step input of magnitude A, if the corresponding response $y(t)$ is bounded, then equation (8) with s replaced by $j\omega$ reduces to

$$G(j\omega) = \frac{1}{A}\int_0^{t_y} y'(t)\,e^{-j\omega t}\,dt \tag{9}$$

where t_y is the duration of the response. Using Euler's relationship, equation (9) can be resolved into magnitude ratio and phase angle to yield the experimental frequency response as

$$|G(j\omega)| = (Re^2 + Im^2)^{1/2}; \quad G(j\omega) = \tan^{-1}(Im/Re) \tag{10}$$

where

$$Re = \frac{1}{A}\int_0^{t_y} y'(t)\cos\omega t\,dt$$

and

$$Im = \frac{1}{A}\int_0^{t_y} y'(t)\sin\omega t\,dt.$$

A detailed discussion on the digital evaluation of these expressions along with an analysis of the accuracy and reliability of the computing procedure involved may be found in [10].

Using the above technique, the transient heat pipe data of this investigation were converted to frequency

response and compared with theoretical predictions (equation 6) in the frequency domain. Results of this comparison along with a discussion on experimental heat pipe dynamics are given below.

RESULTS AND DISCUSSION

Extensive transient data corresponding to step disturbances at the heater input were obtained in the form of millivolt signals using the experimental setup and procedure described earlier. The recordings were then converted to corresponding vapor temperatures (a typical response shown in Fig. 2) and the Fourier transforms extracted by the previously developed data reduction procedure [10]. It was observed during experimentation that replicate runs using different step magnitudes, reduced to such frequency responses, were in good agreement showing that the system was linear at the operating points. Besides, repetitive tests also produced essentially identical results. In what follows representative results, which elucidate the experimental dynamics, are discussed and compared with theory. Most of these data pertain to natural cooling at the condenser end. Additional results corresponding to 72 experiments covering important system and operating parameters may be found in [11].

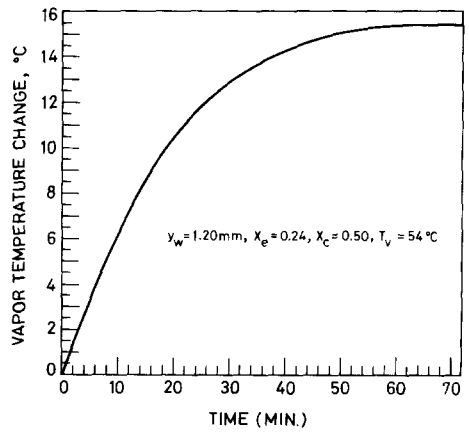

FIG. 2. Typical experimental step response data.

Effect of condenser length

Illustrative vapor temperature responses in the frequency domain, plotted as magnitude ratio and phase angle as functions of frequency, are shown in Fig. 3. The results correspond to three condenser lengths (namely 26, 50 and 76% of the total heat pipe length) for a system equipped with a wick of 0.25 mm thickness and operating at a temperature level of 54°C. The graph shows that the heat pipe responds faster with bigger condenser section substantiating our previous theoretical deduction [7]. The result (see phase data) further displays two distinct zones: (i) a first order dynamics in the low frequency region with the corner frequency varying proportional to the condenser size, and (ii) a distributed parameter behaviour in the high frequency zone that is free from the condenser effect (as evidenced by the data points merging in this

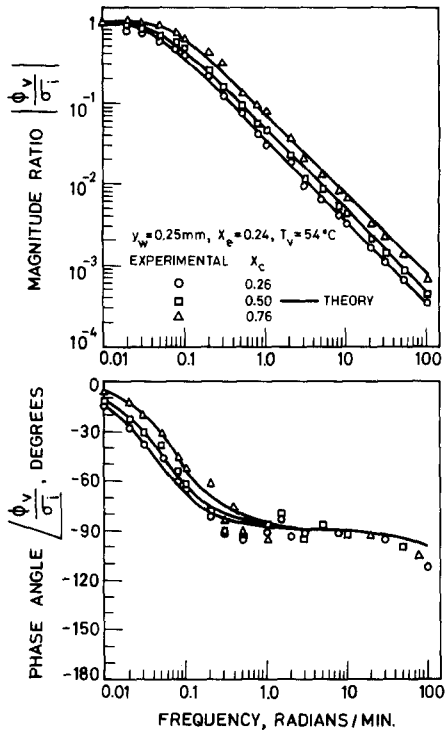

FIG. 3. System frequency response—effect of condenser size.

region). The theoretical magnitude and phase curves corresponding to the experimental conditions, as calculated from equation (6), are also plotted as solid lines in the same graph. The general agreement between experimental data and theoretical prediction is good which reflects on the success of the model in representing the actual system behaviour.

Effect of evaporator length

Evaporator length variation, unlike that of the condenser, does not alter the vapor temperature response. This is shown in Fig. 4 where frequency response data obtained for two different evaporator lengths (i.e. 24 and 50% of the total length) are found to coincide throughout the entire frequency spectrum. An explanation for this on the basis of the boundary conditions imposed is given in [7]. The above observation may also be explained by considering the zero frequency gain expression relating vapor temperature to heat input. Thus, the final steady state value of the vapor temperature, $\phi_v(\infty)$, for a unit step in heat inflow can be derived from equation (6) as

$$\phi_v(\infty) = \frac{1}{X_c}[\eta_m + R(1-\eta_m) + 1/N_{Bi}]. \quad (11)$$

Equation (11), when converted to its dimensional form, yields the vapor temperature as deviation from its initial value as

$$T_v(\infty) = \frac{Q_s}{\pi d_o}\left[\frac{y_m}{L_c K_m} + \frac{(y_t - y_m)}{L_c K_w} + \frac{1}{L_c h_c}\right]. \quad (12)$$

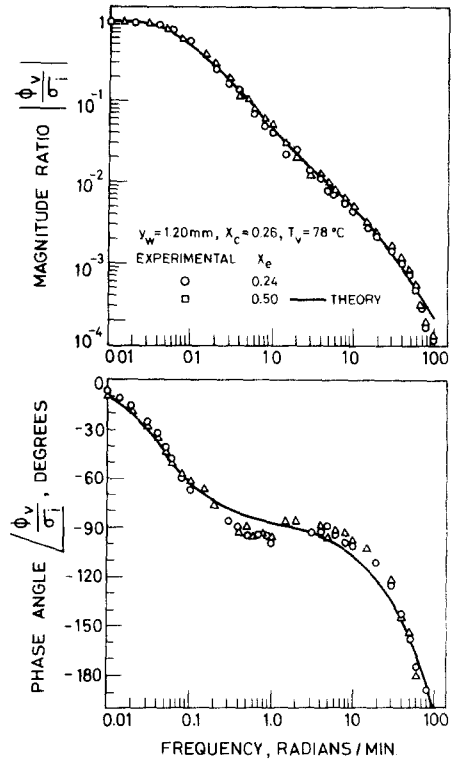

FIG. 4. System frequency response—effect of evaporator size.

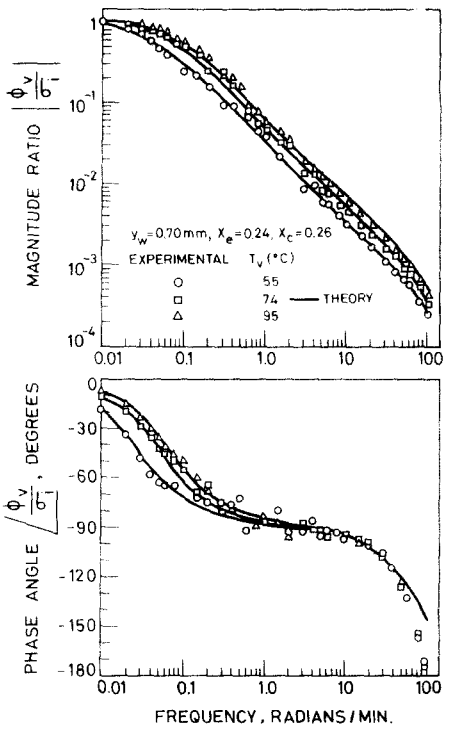

FIG. 5. System frequency response—effect of operating temperature.

In equation (12) the evaporator side parameters are conspicuous by their absence indicating that the vapor temperature is dependent on the condenser length only. Besides, the resistance to heat transfer (terms within the bracket in equation 12) and through it the equivalent first order time constant are seen to be inversely proportional to the condenser length.

Effect of operating temperature

Figure 5 records the experimental responses obtained for three different operating temperatures, viz., 55, 74 and 95°C. The reduced transient (faster dynamics) at higher temperature results mainly from increased heat transfer coefficient, h_c, between the system and the sink. The low frequency region of the magnitude ratio plot indicates that the corner frequency is proportional to the heat-transfer coefficient. Thus, the three experimental corner frequency values, namely 0.03, 0.05 and 0.06 rad/min, are nearly in the same proportion as the corresponding observed heat-transfer coefficients, viz., 0.02, 0.034 and 0.044 cal/min cm^2 °C. The way the phase data points in Fig. 5 converge at elevated frequencies indicates that the influence of temperature on dynamics is restricted to low frequency region only. The figure, in addition, provides further confirmation to the correspondence between experimental and analytical results. It may also be observed here that other factors which affect the heat-transfer coefficient (such as circulation rate of the coolant and emissivity of the heat pipe surface) will have the same influence on the dynamics as the temperature.

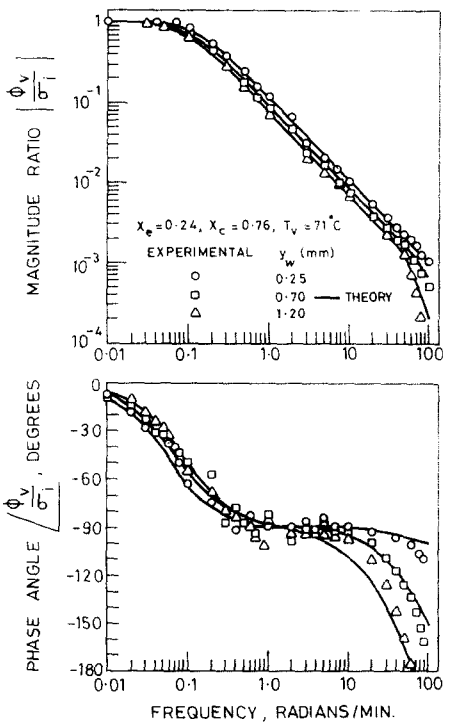

FIG. 6. System frequency response—effect of wick thickness.

Effect of wick thickness

Figure 6 presents illustrative system frequency response as a function of wick thickness. In contrast to the previous parameters which exercised considerable influence on the low frequency system dynamics, wick

thickness alters the high frequency response characteristics as revealed better in the phase plot rather than in magnitude data. The sharp increase observed in phase lag with wick thickness at higher frequencies is an indication of deterioration in system dynamics with the wick property. This is caused by increase in thermal capacitance and resistance inside the heat pipe due to higher wick thicknesses. The relatively more deviation of the experimental data points at higher frequencies is typical. This is due to the limited accuracy of the original record to which the phase angle is known to be sensitive. It may be noted that, since thermal conductivity and heat capacity of the liquid-filled wick also govern the internal thermal resistance and capacitance, variations in these properties would also produce identical results.

Effect of forced cooling

In all the cases discussed above, heat rejection was achieved by natural convection. Hence, for the sake of illustration, some experimental results are presented here (Fig. 7) for a system equipped with a water-cooled jacket of length 16 cm. The response in this case can be seen to be similar to that obtained with natural cooling; however, it is faster owing to the increased heat-transfer coefficient due to forced convection.

CONCLUSIONS

To conclude, detailed frequency response data, hitherto not available, have been procured for a range of system and operating parameters using a number of heat pipes. The experimentation involved procuring step response data relating vapor temperature to heat input and converting them to frequency form via the procedure developed earlier [10]. The results obtained clearly describe and differentiate the effects of system parameters on the dynamics. Of particular interest are the observations that the high frequency response characteristics are entirely determined by the wick parameters, whereas the low frequency dynamics are governed by the condenser parameters and operating temperature.

The experimental values of magnitude ratio and phase angle closely agree with theoretical predictions thereby validating the proposed theory.

In addition, ten thousand fold coverage (four decades) of experimental frequency response achieved reflects on the efficiency of the time-to-frequency domain conversion method employed.

Apart from describing the dynamics, the results of this analysis could be used in designing control systems for heat pipes.

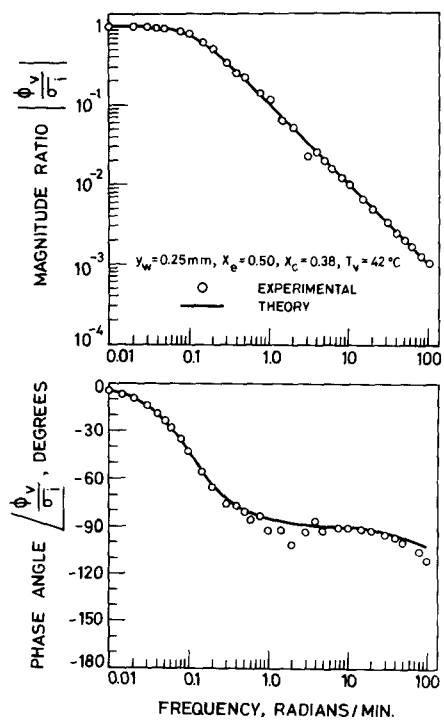

FIG. 7. Frequency response for a system with forced cooling.

REFERENCES

1. J. O. Hougen, Experiences and experiments in process dynamics, *Chem. Engng. Prog. Monogr. Ser.* **60** (4) (1964).
2. M. Gröll and P. Zimmermann, Das stationäre und instationäre Betviebsverhalten von Wärmerohren, *Wärme-und Stoffübertragung* **4**, 39–47 (1971)
3. J. E. Deverall, J. E. Kemme and L. W. Florschuetz, Sonic limitations and startup problems of heat pipes, Los Alamos Scientific Lab. Rep. No. LA-4518 (1970).
4. S. W. Kessler, Jr., Transient thermal impedance of a water heat pipe, Paper No. 71-WA/HT-9, in *ASME Winter Annual Heat Transfer Conference*, Washington, D.C. (1971).
5. B. D. Marcus and G. L. Fleischman, Steady state and transient performance of hot reservoir gas-controlled heat pipes, Paper No. 70-HT/SpT-11, in *ASME Space Technology and Heat Transfer Conference*, Los Angeles (1970).
6. G. Rice and E. Azad, Dynamic characteristics of heat pipes, in *Proceedings of the Second International Heat Pipe Conference*, Vol. 1, pp. 153–164. European Space Agency Publication, The Netherlands (1976).
7. A. Rajakumar and P. R. Krishnaswamy, Transfer function analysis of heat pipes, *Proceedings of the Second International Heat Pipe Conference*, Vol. 2, pp. 761–772. European Space Agency Publication, The Netherlands (1976).
8. J. O. Hougen and R. A. Walsh, Pulse testing, *Chem. Engng. Prog.* **57**, 69–79 (1961).
9. W. C. Clements and K. B. Schnelle, Pulse testing for dynamic analysis, *I/EC Process Des. Dev.* **2**, 94–102 (1963).
10. A. Rajakumar and P. R. Krishnaswamy, Time to frequency domain conversion of step response data, *I/EC Process Des. Dev.* **14**, 250–256 (1975).
11. A. Rajakumar, Step testing of heat pipes, Ph.D. Thesis, Indian Institute of Technology, Madras (1975).
12. J. H. Cosgrove, Engineering design of heat pipes, Ph.D. Thesis, North Carolina State University (1967).
13. R. L. Gorring and S. W. Churchill, Thermal conductivity of heterogeneous materials, *Chem. Engng. Prog.* **57** (7), 53–59 (1961).
14. W. L. Haskin, Cryogenic heat pipe, Air Force Flight Dynamics Lab. Tech. Report No. AFFDL-TR-66-228 (1967).
15. H. R. Kunz, S. S. Wyde, G. H. Nashick and J. F. Branes, Vapor-chamber fin studies—operating characteristics of fin model, NASA CR-1139 (1968).
16. B. D. Marcus, Theory and design of variable conductance heat pipes, NASA CR-2018 (1972).

DYNAMIQUE EXPERIMENTALE ET FREQUENTIELLE DES CALODUCS

Résumé—Des essais de réponse en fréquence ont été menés sur plusieurs caloducs à eau avec des écrans de bronze fritté comme mèches. L'expérimetation consiste à soumettre les tubes de chaleur à un changement échelon du flux de chaleur et à convertir le temps de réponse en données fréquentielles à partir de la transformation de Fourier. Des variations de paramètres tels que la température, la surface du condenseur, celle de l'évaporateur et l'épaisseur de la mèche sont considérées pour étudier leurs effets sur la dynamique de système. Les résultats obtenus sont comparés à une théorie proposée. En plus d'une information quantitative sur un domaine de fréquence jusqu'ici indisponible, les résultats dégagent l'influence des variables expérimentales sur la dynamique.

EXPERIMENTELLE UNTERSUCHUNG DES DYNAMISCHEN VERHALTENS VON WÄRMEROHREN IM FREQUENZBEREICH

Zusammenfassung—Aus Versuchen mit einer Anzahl von Wasser-Wärmerohren mit eingepreßtem Bronze-Gitter als Dochtmaterial wurden ausführliche Frequenzgang-Daten gewonnen. Im Verlauf der Untersuchungen wurden die Wärmerohre einer springförmigen Veränderung der Wärmezufuhr unterworfen; die gewonnene Sprungantwort wurde mittels Fourier-Transformation vom Zeitbereich in den Frequenzbereich übertragen. Einzelne Parameter, wie z. B. die Arbeitstemperatur, Kondensatorfläche, Verdampferfläche und die Dicke des Dochtes, wurden variiert, um ihre Auswirkung auf das dynamische Verhalten des Systems zu erkennen. Die erzielten Ergebnisse wurden mit einer vorgeschlagenen Theorie verglichen mit dem Ziel, letztere zu bestätigen. Neben der Lieferung quantitativer Aussagen über das bisher noch nicht beschriebene dynamische Verhalten im Frequenzbereich geben die Ergebnisse auch Aufschluß über den Einfluß der Versuchsvariablen auf das dynamische Verhalten.

ДИНАМИКА ЭКСПЕРИМЕНТАЛЬНОЙ ЧАСТОТНОЙ ХАРАКТЕРИСТИКИ ТЕПЛОВЫХ ТРУБ

Аннотация — Получены подробные экспериментальные данные о частотных характеристиках ряда тепловых труб на воде, в которых в качестве фитиля используется спресованная бронзовая сетка. В эксперименте подвод тепла к тепловым трубам изменялся ступенчатым образом, а временные характеристики преобразовывались в частотные по методу Фурье. Изменения таких параметров, как рабочая температура, площадь конденсатора, площадь испарителя и толщина фитиля, производились с целью исследования их влияния на динамику системы. Полученные экспериментальные данные сравнивались с теоретическими результатами для подтверждения предложенной теории. Полученные данные представляют собой количественную информацию о ранее неизученной динамике частотных характеристик. Кроме того, они позволили выявить влияние на динамику переменных экспериментальных величин.